38. Zhu X et al. *Phys. Rev. Lett.* **74** 1633 (1995)
39. Yoshioka D, MacDonald A H *J. Phys. Soc. Jpn.* **59** 4211 (1990)
40. Chen X M, Quinn J J *Phys. Rev. Lett.* **67** 895 (1991)
41. Fernández-Rossier J, Tejedor C *Phys. Rev. Lett.* **78** 4809 (1997)
42. Lozovik Yu E, Berman O L *Zh. Eksp. Teor. Fiz.* **111** 1879 (1997) [*JETP* **84** 1027 (1997)]
43. Liu L, Świerkowski L, Neilson D *Physica B* **249 – 251** 594 (1998)
44. Lozovik Yu E, Ovchinnikov I V *Pis'ma Zh. Eksp. Teor. Fiz.* **74** 318 (2001) [*JETP Lett.* **74** 288 (2001)]
45. Larionov A V et al. *Pis'ma Zh. Eksp. Teor. Fiz.* **75** 689 (2002) [*JETP Lett.* **75** 570 (2002)]
46. Dremin A A et al. *Pis'ma Zh. Eksp. Teor. Fiz.* **76** 526 (2002) [*JETP Lett.* **76** 450 (2002)]
47. Timofeev V B et al. *Phys. Rev. B* **60** 8897 (1999)
48. Gorbunov A V, Timofeev V B, Bisti V E *Zh. Eksp. Teor. Fiz.* (2005) (in press)
49. Gorbunov A V, Timofeev V B *Pis'ma Zh. Eksp. Teor. Fiz.* **80** 210 (2004) [*JETP Lett.* **80** 185 (2004)]
50. Butov L V, Gossard A C, Chemla D S *Nature* **418** 751 (2002)
51. Butov L V et al. *Phys. Rev. Lett.* **92** 117404 (2004)
52. Snoke D et al. *Nature* **418** 754 (2002); Snoke D *Science* **298** 1368 (2002)
53. Rapaport R et al. *Phys. Rev. Lett.* **92** 117405 (2004)
54. Lerner I V, Lozovik Yu E *Zh. Eksp. Teor. Fiz.* **78** 1167 (1980) [*Sov. Phys. JETP* **51** 588 (1980)]
55. Butov L V et al. *Phys. Rev. Lett.* **87** 216804 (2001)
56. Lozovik Yu E et al. *Phys. Rev. B* **65** 235304 (2002)

PACS numbers: **42.65. – k**, **71.36. + c**, **78.65. – n**
DOI: 10.1070/PU2005v048n03ABEH002125

Hard excitation of stimulated polariton – polariton scattering in semiconductor microcavities

N A Gippius, S G Tikhodeev,
L V Keldysh, V D Kulakovskii

In recent years, unusual properties of polariton – polariton scattering of light in semiconductor microcavities have attracted continual attention [1 – 12]. In particular, it has been shown in experiment [13] [1] that as the resonant excitation frequency departs from the inflection point of the lower polariton branch (LPB), the scattered signal above the stimulated scattering threshold is always directed roughly perpendicularly to the microcavity (MC) plane. However, based on the simple four-wave mixing model [7], the signal should be expected to shift along the lower polariton branch (see the scattering diagram in Fig. 1).

This inference has recently been confirmed in [15]. Such behavior was theoretically explained in Refs [16 – 19] in terms of the interplay between two instabilities: bistability of the response of the polariton mode to an external pump and the parametric instability of this mode relative to the decay into scattered polaritons. The bistability of the linear optical response when the pump is normal to the surface of the microcavity (in the region of the LPB minimum) was demonstrated in a recent work [20]. However, the mutual influence of bistability and parametric instability feasible in the case of pump near the inflection point of the LPB gives rise to totally new and unexpected nonlinear effects. The aim of this paper is to discuss the physical interpretation of the instabilities found in Refs [16 – 19] and to analyze effects of quasi-two-dimensionality of polariton – polariton scattering and the saturation of excitonic transitions. We emphasize that from the quantum standpoint, macro-occupied polariton modes whose behavior is considered below obey the Bose statistics. Hence, we actually discuss the kinetics of a strongly nonequilibrium Bose system.

It is widely accepted that stimulated scattering commences softly (in analogy with the soft generator excitation regime) as the system loses stability for certain scattered modes when the threshold is exceeded. Such modes become macro-occupied as the threshold is passed over smoothly, and their amplitude gradually increases with the pump. Because the macro-occupied modes grow slowly (due to a small growth increment of unstable modes near the threshold), they effectively suppress the accumulation of the scattered signal in the nearby modes with a smaller incremental growth. Simultaneously, the pump mode amplitude is stabilized by the incoming energy balance. Such behavior is reminiscent of a *second*-order phase transition that occurs in a nonequilibrium system under the effect of external excitation, when the entire system passes concertedly and smoothly to a more stable macroscopic state.

Studies [17 – 19] have demonstrated that stimulated scattering of excitonic polaritons in a semiconductor MC can arise in a 'hard' manner (by analogy to the hard generator excitation regime). In this case, the amplitude of an *excited* polariton mode initially increases in a jump due to its bistability typical of nonlinear oscillators. If such transformation of the excited mode results in the system falling in the region of strong instability with respect to polariton – polariton scattering (or any other scattering, e.g., on phonons or free carriers), the corresponding modes in a large phase space region are characterized by substantial growth increments and start to be populated explosively. The incoming energy balance makes the population of the excited mode decrease abruptly, and the scattered signal is strongly stochastic. This behavior is similar to the *first*-order phase transition that occurs in a nonequilibrium system excited from the outside. Although the system in Refs [17 – 19] is assumed to be spatially uniform, one can expect its stratification into spatially inhomogeneous regions. It is worth noting that the bistability-allowed possibility of the nonlinear spatially inhomogeneous self-organization of the scattered signal has recently been considered theoretically in the framework of a similar approach in Ref. [21]. The same approach was applied in another recent work [22] to clarify the feasibility of superfluidity in the polariton system in a microcavity.

The process of polariton parametric scattering is illustrated by Fig. 1. The theoretical analysis of its development includes the consideration of semiclassical equations for $\mathcal{E}_{\mathrm{QW}}$, the quantum well (QW) electric field in a microcavity, and for the exciton polarization $\mathcal{P}(k,t)$ averaged over the QW width [19]:

$$\left[\mathrm{i}\frac{\mathrm{d}}{\mathrm{d}t} - E_{\mathrm{C}}(k)\right]\mathcal{E}_{\mathrm{QW}}(k,t) = \alpha(k)\mathcal{E}_{\mathrm{ext}}(k,t) + \beta(k)\mathcal{P}(k,t)\,, \quad (1)$$

$$\left[\mathrm{i}\frac{\mathrm{d}}{\mathrm{d}t} - E_{\mathrm{X}}(k)\right]\mathcal{P}(k,t)$$

$$= A\sum_{q,q'}\left[\delta_{q,k} - V_{\mathrm{sat}}\mathcal{P}(q',t)\,\mathcal{P}^*(q+q'-k,t)\right]\mathcal{E}_{\mathrm{QW}}(q,t)$$

$$+ F\sum_{q,q'}\mathcal{P}(q',t)\,\mathcal{P}^*(q+q'-k,t)\,\mathcal{P}(q,t) + \xi(k,t)\,. \quad (2)$$

[1] See also the next report [14] in this issue.

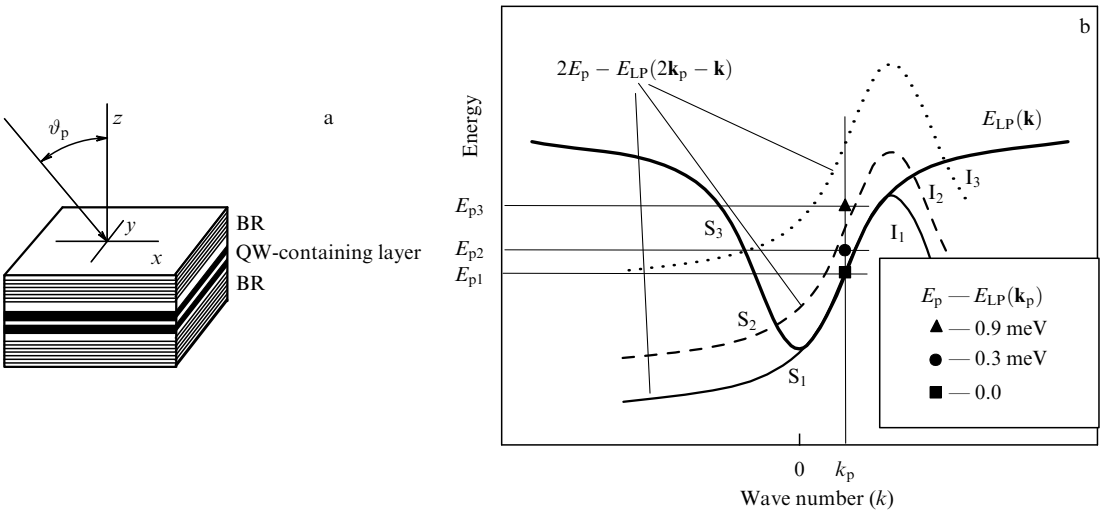

Figure 1. (a) Schematic representation of light scattering in a planar microcavity made of λ or $3/2\lambda$ layers (λ is the resonant wavelength) containing quantum wells (QW) and enclosed between distributed Bragg reflectors (BR). (b) Schematic of polariton–polariton scattering at a low pump intensity. The thick solid curve shows the lower polariton branch $E_{LP}(\mathbf{k})$. The thin curves (solid, dashed, and dotted) correspond to the idle modes $2E_p - E_{LP}(2\mathbf{k}_p - \mathbf{k})$ for several detunings between the pump frequency and the lower polariton branch $E_p - E_{LP}(\mathbf{k}_p)$ (square, circle, and triangle). By virtue of energy and momentum conservation, the maximum scattering occurs for the energies and momenta at the points of intersection of the curves $E_{LP}(\mathbf{k})$ and $2E_p - E_{LP}(2\mathbf{k}_p - \mathbf{k})$. Hence, in the framework of this model, it is natural to expect shifts in the signal $S_1 \to S_2 \to S_3$ and the idler $I_1 \to I_2 \to I_3$ along the lower polariton branch with increasing pump detuning $E_{p1} \to E_{p2} \to E_{p3}$.

Here, $\mathcal{E}_{ext} = \mathcal{E}(t)\exp(-iE_p t)\,\delta(k - k_p)$ is the electric field of the incident pump electromagnetic wave far away from the MC, described as a macro-occupied photon mode with a fixed frequency E_p, the wave number $k_p = E_p \sin\vartheta/c$, and the time-variable amplitude $\mathcal{E}(t)$. E_C and E_X are the resonance frequency of an empty MC and the exciton frequency in a free QW, respectively, F is the exciton–exciton coupling constant, A is the exciton polarizability, $\xi(k,t)$ is the Langevin random force with $\langle\xi(k,t)\rangle = 0$ and $\langle\xi(k,t)\,\xi(k',t')\rangle \propto \delta(k-k')\,\delta(t-t')$. The microcavity response constants α and β are calculated by the scattering matrix method [23]. The energy is measured in millielectronvolts and the polarization and electric field in such units that $F = 1$.

Equation (1) is the Maxwell equation written in the resonant scalar approximation (i.e., with the $\sigma^{\pm}$-polarizations ignored) with the exciton polarization taken into account. Equation (2) is the inhomogeneous nonlinear Schrödinger equation for excitonic polarization that includes two types of sources, a coherent external excitation and a stochastic Langevin noise. The latter makes it possible to simulate quantum fluctuations of the scattering signal using semiclassical equations (1) and (2).

Equations (1) and (2), unlike those considered in Refs [17, 18] (see also report [14] below), contain an additional term (with the coefficient V_{sat}) that describes saturation of the excitonic transition. Strictly speaking, a full account of saturation requires solving a system of equations for the electron–hole density matrix that relates diagonal elements of the matrix to the dynamics of nondiagonal elements describing coherent polarization. Here, we use a simplified approach [24] in which a nonlinear term proportional to $|\mathcal{P}(x)|^2\mathcal{E}(x)$ is introduced in the equation for QW-averaged exciton polarization (2). The system of equations thus written assumes that the field and polarization system dynamics are on the whole fairly well described by nondiagonal components of the density matrix only.

With this approximation in mind, we now demonstrate that at $V_{sat} \lesssim 0.1$, the saturation of the exciton transition results in no qualitative change in the scattering pattern and is actually reduced to an additional linear blue-shift of the lower polariton branch. The introduced parameter V_{sat} describes the relative saturation of the exciton transition [3, 20]. For GaAlAs-microcavities, the parameter V_{sat} is a small number, $V_{sat} \approx 0.1$.[2] This agrees with the well-established fact that the exciton collisional nonlinearity regime occurs at intensities below the saturation threshold for the excitonic transition.

The nonlinear Schrödinger equation takes only the contact exciton–exciton coupling into account. The model does not include, for example, the exciton–phonon interaction that can play an important role in the processes of parametric scattering of MC polaritons. However, even in this simplest approximation, the model turns out to exhibit a threshold behavior [16–18] qualitatively similar to that observed in experiment [13]. The threshold pump values thus obtained lie in the range 10^2–10^3 W cm^{-2}, i.e., they are of the same order of magnitude as the experimental values.

An example of the threshold behavior of Eqns (1) and (2) discovered by us is presented in Figs 2 and 3. In the numerical simulation, the scattering was for simplicity assumed to be quasi-one-dimensional (only in the pump incidence plane), and the shape of the pump pulse $\mathcal{E}_{ext}(t)$ (shown by the dashed-dotted line in the inset to Fig. 2) was chosen such that the pump intensity threshold could be smoothly reached during the exciting pulse. Specifically, the pump amplitude $\mathcal{E}_{ext}(t)$ was first switched on to 97% of its maximum for about 100 ps, then increased slowly to the maximum value for $\sim$ 1000 ps, and finally switched off within another 100 ps. It follows from the figure that the system's kinetics was characterized by two abrupt transitions at $t \approx 600$ and 700 ps. Both transitions were associated with a sharp change of polarization of the

[2] Although not as small as the estimate 10^{-2} reported in Ref. [20].

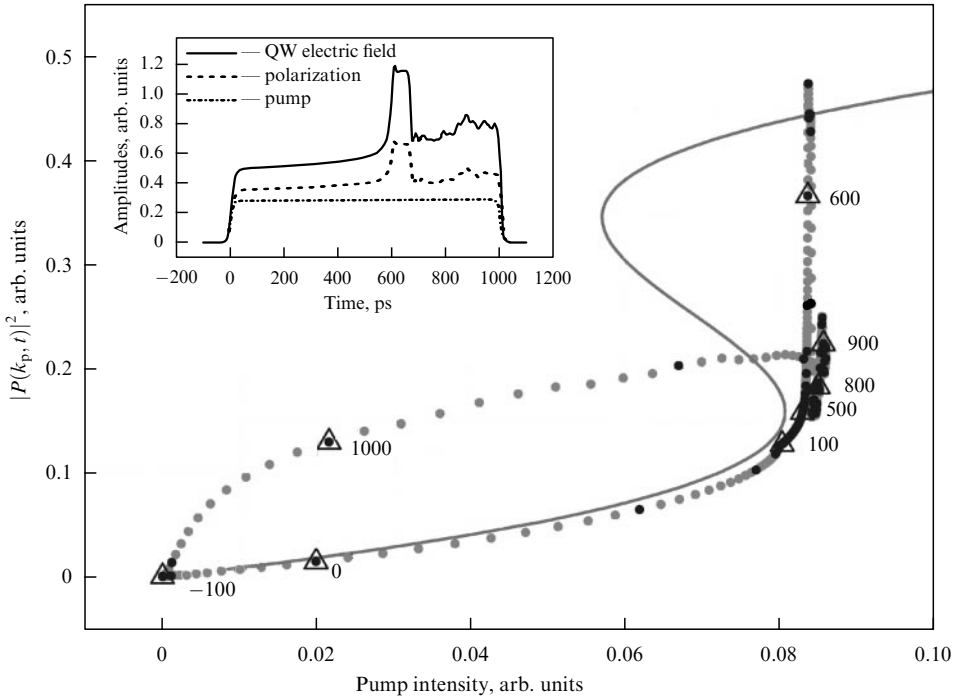

Figure 2. The trajectory of polarization of the pumped polariton mode in the coordinates '|exciton polarization|^2 — external pump'. The time delay between the grey (black) points is 1 ps (10 ps), time instants corresponding to the triangles are given near them in picoseconds. The solid S-shaped curve is the solution of Eqn (5) for a stationary external pump. The inset shows time variations of the QW electric field amplitude (solid curve), the exciton polarization amplitude (dotted curve), and the amplitude of the external pump field (dashed-dotted curve). Evidently, the system undergoes two abrupt transitions at $t \approx 600$ and 700 ps under virtually unaltered pump.

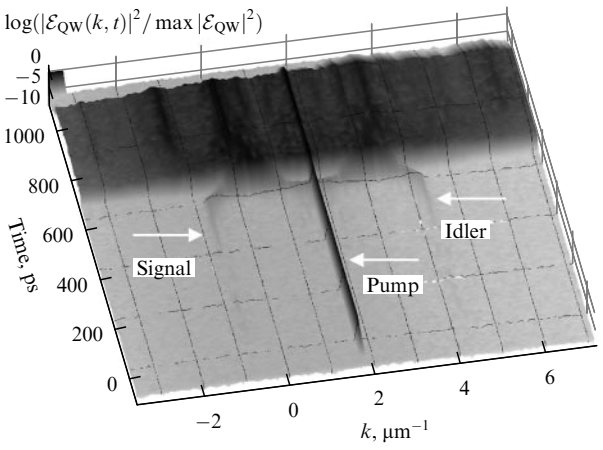

Figure 3. Numerically evaluated time variation of the spatial harmonics of the QW electric field in a microcavity. This quantity normalized to its maximum value is plotted along the vertical in a logarithmic scale and is also shown by grayscale (see the vertical scale): black colors indicate higher intensities. The exciting wave (pump) is incident at the angle 14° corresponding to the momentum $k_p \approx 1.9$ μm^{-1}. We note that at $t \lesssim 600$ ps, i.e., prior to the first transition, the signal and the idler have maximum values at $k_s < 0$ and $k_i > 2k_p$, respectively. Following the second transition at $t \approx 700$ ps, the maxima are shifted towards $k_s \gtrsim 0$ and $k_i \lesssim 2k_p$, while the average intensity of the scattered modes with $k \neq k_p$ increases by five to six orders of magnitude.

pumped polariton mode $\mathcal{P}_0$ and the corresponding spatial harmonic of the QW electric field $\mathcal{E}_0$ (solid and dotted lines in Fig. 2, respectively).

The above transitions are accompanied by a rise in the total intensity of the scattered polariton signal by many orders of magnitude (see Fig. 3 showing the time and wave number dependences of the scattered polariton signal). It can be seen from Fig. 3 that the maxima of the signal and idler before the first transition with $t \approx 600$ ps are positioned in excellent agreement with the four-wave mixing theory [7, 8]. In other words, for a positive pump detuning (the pump quantum energy higher than the LPB energy at the pump wave number as shown in Fig. 1), the signal and the idler have maxima at $k_s < 0$ ($\vartheta_s < 0$) and $k_i > 2k_p$, respectively.

To understand the nature of the abrupt transitions demonstrated by the numerical solutions of Eqns (1) and (2), it is necessary to study [18, 19] the stability of their solutions at the steady-state external pump $\mathcal{E}_{ext}(t) = \text{const}$ and with a single micro-occupied mode, i.e., in the form

$$\mathcal{P}(k,t) = \tilde{\mathcal{P}}(k,t) + \delta_{k,k_p}\mathcal{P}_0 \exp(-iE_p t)\,, \tag{3}$$

$$\mathcal{E}_{QW}(k,t) = \tilde{\mathcal{E}}(k,t) + \delta_{k,k_p}\mathcal{E}_0 \exp(-iE_p t)\,. \tag{4}$$

Here, $\tilde{\mathcal{P}}$ and $\tilde{\mathcal{E}}$ are assumed to be small deviations from the solution with one micro-occupied mode $|\tilde{\mathcal{P}}/\mathcal{P}_0|, |\tilde{\mathcal{E}}/\mathcal{E}_0| \ll 1$.

In the zero order in $\tilde{\mathcal{P}}$ and $\tilde{\mathcal{E}}$, a cubic equation is obtained [19] for the amplitude of the excited mode $\mathcal{P}_0$,

$$(\Delta_{PC}\,\Delta_{PX} - \tilde{A}\beta)\mathcal{P}_0 - \Delta_{PC}F|\mathcal{P}_0|^2\mathcal{P}_0 = \tilde{A}\alpha\mathcal{E}_{ext}\,, \tag{5}$$

where

$$\tilde{A} = A(1 - V_{sat}|\mathcal{P}_0|^2)\,, \qquad \Delta_{PC} = E_p - E_C(k_p)\,,$$
$$\Delta_{PX} = E_p - E_X(k_p)\,.$$

This dependence, starting from certain positive detuning values, has an S-shape as shown in Fig. 4 for the absence of

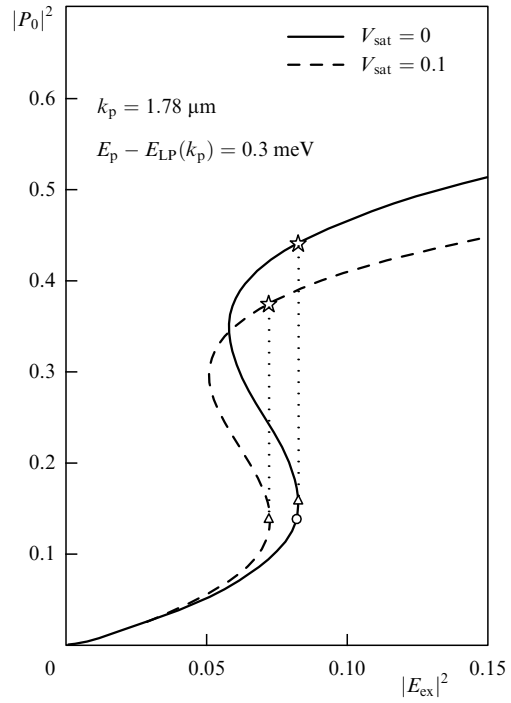

Figure 4. S-shaped curve of a driven nonlinear excitonic oscillator in the coordinates '|exciton polarization|^2 — external pump' computed without regard for the saturation of the exciton transition (solid curve as in Fig. 2) and taking the saturation at $V_{sat} = 0.1$ into account (dashed curve). The open circle on the solid S-curve indicates parameters corresponding to the parametric instability threshold. The triangles show the points of the lost stability of the lower branch of the S-curve; renormalized spectra at these points are shown in Figs 5a, b and 6a, b. The star symbols indicate the states of the system with a high polariton density on the upper branch of the S-curve; the corresponding renormalized spectra are presented in Figs 5c, d and 6c, d.

saturation, $V_{sat} = 0$ (solid curve) and for $V_{sat} = 0.1$ (dashed curve). The S-shaped curve for $V_{sat} = 0$ is also depicted in Fig. 2.

Such S-curves were investigated in the theory of 'empty' nonlinear microcavities with a Kerr nonlinearity without resonant excitons in QWs (see, e.g., Refs 25–27). As regards the existence of S-shaped dependences, the absolute instability of the solution of Eqn (5) in the region where the derivative $d\mathcal{P}_0/d\mathcal{E}_{ext}$ is negative leads to the bistability of the response of a nonlinear oscillator, as is perfectly well known, after the work of Duffing [28] at least (see reviews [29, 30]). It should be noted that in early theoretical studies of polariton–polariton scattering in a MC [3, 7–9, 11] the driving parameter was considered to be the amplitude of the pumped mode polarization (rather than the external electric field far from the cavity); therefore, bistability could not develop in principle. Such an approximation, justified at small detunings from the LPB (when no S-shaped dependence arises), leads to incorrect predictions at large detunings. The importance of bistability for MCs with polaritons [20–22, 31] has been perceived only in recent years, after publications [16–18].

We now consider the conditions of stability of the solution with a single macro-occupied mode (5). For this, we linearize Eqns (1) and (2) with respect to small deviations of the signal amplitude

$$\tilde{\mathcal{E}}(k,t) = \tilde{\mathcal{E}}(k)\exp(-i\omega t), \qquad \tilde{\mathcal{P}}(k,t) = \tilde{\mathcal{P}}(k)\exp(-i\omega t)$$

and the idler amplitude

$$\tilde{\mathcal{E}}^*(\bar{k},t)\exp(-2iE_p t) = \bar{\tilde{\mathcal{E}}}(\bar{k})\exp(-i\omega t),$$
$$\tilde{\mathcal{P}}^*(\bar{k},t)\exp(-2iE_p t) = \bar{\tilde{\mathcal{P}}}(\bar{k})\exp(-i\omega t),$$

where $\bar{k} = 2k_p - k$,

$$\omega \begin{pmatrix} \tilde{\mathcal{E}}(k) \\ \tilde{\mathcal{P}}(k) \\ \bar{\tilde{\mathcal{E}}}(\bar{k}) \\ \bar{\tilde{\mathcal{P}}}(\bar{k}) \end{pmatrix} = \hat{H}_{eff} \begin{pmatrix} \tilde{\mathcal{E}}(k) \\ \tilde{\mathcal{P}}(k) \\ \bar{\tilde{\mathcal{E}}}(\bar{k}) \\ \bar{\tilde{\mathcal{P}}}(\bar{k}) \end{pmatrix}. \tag{6}$$

Here, the effective 'Hamiltonian' is given by a (4×4) matrix [19],

$$\hat{H}_{eff} = \begin{pmatrix} E_C(k) & \beta & 0 & 0 \\ \tilde{A} & E_X + 2F|\mathcal{P}_0|^2 - AV_{sat}\mathcal{P}_0^*\mathcal{E}_0 & 0 & F\mathcal{P}_0^2 - AV_{sat}\mathcal{P}_0\mathcal{E}_0 \\ 0 & 0 & 2E_p - E_C^*(\bar{k}) & -\beta^* \\ 0 & -(F\mathcal{P}_0^2 - AV_{sat}\mathcal{P}_0\mathcal{E}_0)^* & -\tilde{A}^* & 2E_p - (E_X + 2F|\mathcal{P}_0|^2 - AV_{sat}\mathcal{P}_0^*\mathcal{E}_0)^* \end{pmatrix}. \tag{7}$$

Eigenfrequencies $\Omega(k)$ of the linear problem in (6) and (7) can serve as indices of stability of the solution with a single macro-occupied mode (3)–(5). If the imaginary part of the eigenfrequencies $\Omega(k)$ is negative, the solution with one macro-occupied mode (3)–(5) is stable because deviations from it decrease exponentially with time, $\propto \exp[\mathrm{Im}\,\Omega(k)t]$, $\mathrm{Im}\,\Omega(k) < 0$. Otherwise, the growth increment is positive, $\mathrm{Im}\,\Omega(k) > 0$, and the solution is unstable.

Figure 5a, b illustrates the dependences of the eigenfrequencies of linear problem (6), (7) on the two-dimensional wave number calculated for $V_{sat} = 0$ at $|\mathcal{P}_0|^2 = 0.16$, $|\mathcal{E}_{ext}|^2 = 0.083$, i.e., at the terminal right point of the lower stable branch of the S-curve (see the triangle on the solid curve in Fig. 4). Interestingly, the threshold of this instability at the given parameters of the microcavity and pump lies at a slightly larger external field than the boundary of parametric instability (see the circle in Fig. 4 corresponding to $|\mathcal{P}_0|^2 = 0.14$, $|\mathcal{E}_{ext}|^2 = 0.081$). That the parametric instability threshold is passed over is evidenced by the appearance of an eight-shaped instability region of the single-mode solution in Fig. 5b: the imaginary part of the eigenvalue is already positive within this region and the corresponding polariton modes are unstable. At pump intensities somewhat below the parametric instability threshold, the same modes have a maximum lifetime. In the stationary regime, the signal accumulates in these long-lived modes; therefore, the scattered signal intensity is maximum below the threshold, in the directions forming the figure eight. This effect was theoretically predicted in Ref. [7] and was recently demonstrated in experiment [32].

We return to the scattering kinetics depicted in Fig. 2 and compare the evolution of the pumped mode (points and triangles) with the S-shaped curve of the solution with a single macro-occupied mode (solid curve). Evidently, the first abrupt transition at $t \approx 600$ ps is the transition of the driven nonlinear oscillator from the lower to the upper branch of the S-curve. This means that the first instability at $t \approx 600$ ps in

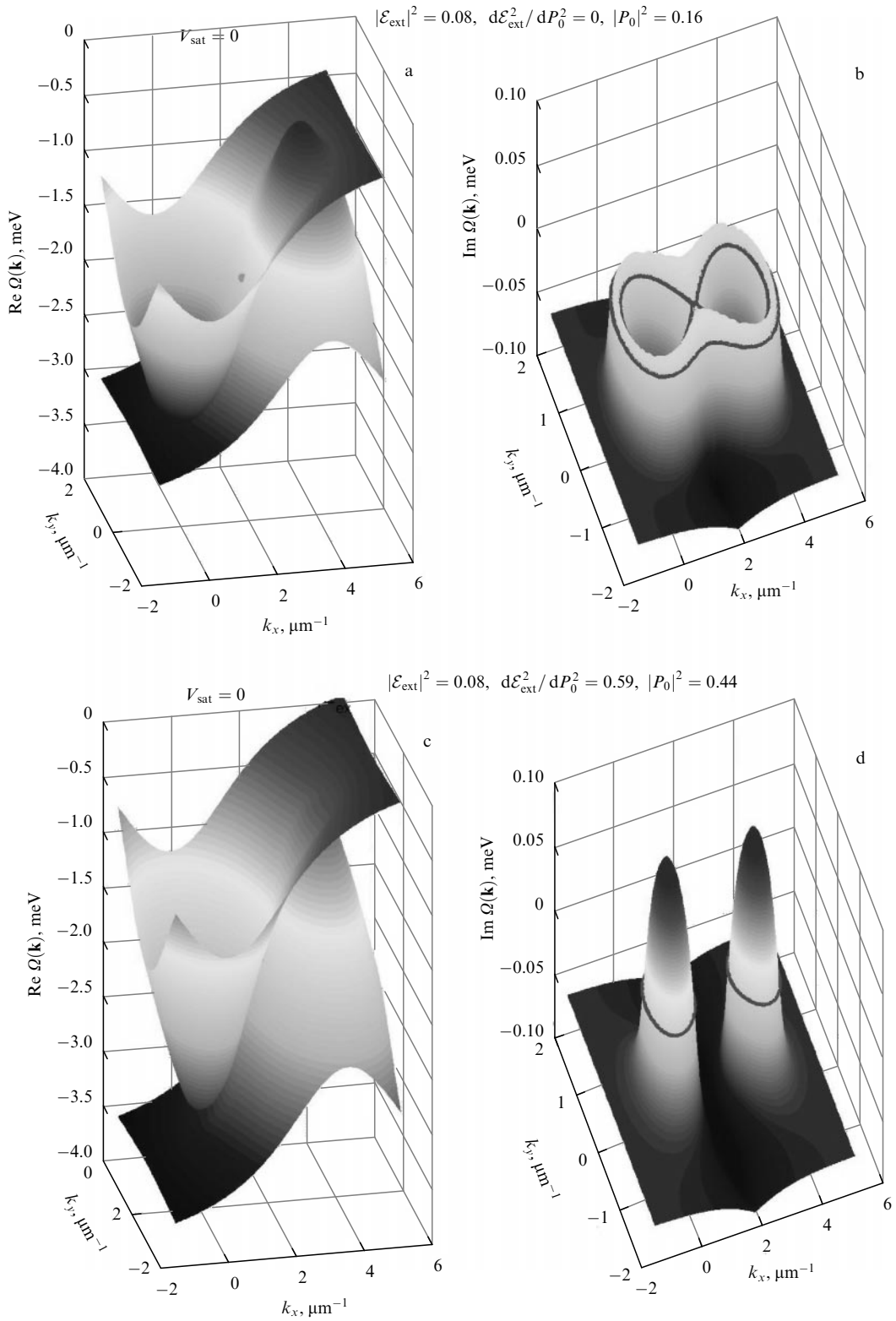

Figure 5. Calculated renormalized spectra of the signal and idler modes $\Omega(\mathbf{k})$ for $V_{\rm sat} = 0$: (a, b) spectra at the point of the lost stability of the lower branch of the S-curve ($|\mathcal{P}_0|^2 = 0.16$, $\mathcal{E}^2_{\rm ext} = 0.083$) (the triangle on the solid S-curve in Fig. 4); (c,d) spectra on the upper branch of the S-curve at the point corresponding to the same external pump $\mathcal{E}^2_{\rm ext} = 0.083$ but with a stronger polarization, $|\mathcal{P}_0|^2 = 0.44$ (the star symbol on the solid S-curve in Fig. 4). Real parts of the renormalized energies of the signal and idler modes $|\mathcal{P}_0|^2 = 0.44$ are shown in Figs a, b. Figures c,d show the imaginary part Re $\Omega(\mathbf{k})$ of only the longest-lived (or unstable) mode. The thick solid contour in Figs c, d is the boundary of the stable region Im $\Omega(\mathbf{k}) = 0$.

the approximation of one-dimensional scattering and in the absence of saturation results from the loss of stability of the solution at the end of the lower stable branch of the S-contour. Because the S-contour is independent of the spatial dimensionality, this instability is also preserved in the quasi-two-dimensional case.

The development of the first instability brings the system into the region of the upper branch of the S-contour (see the

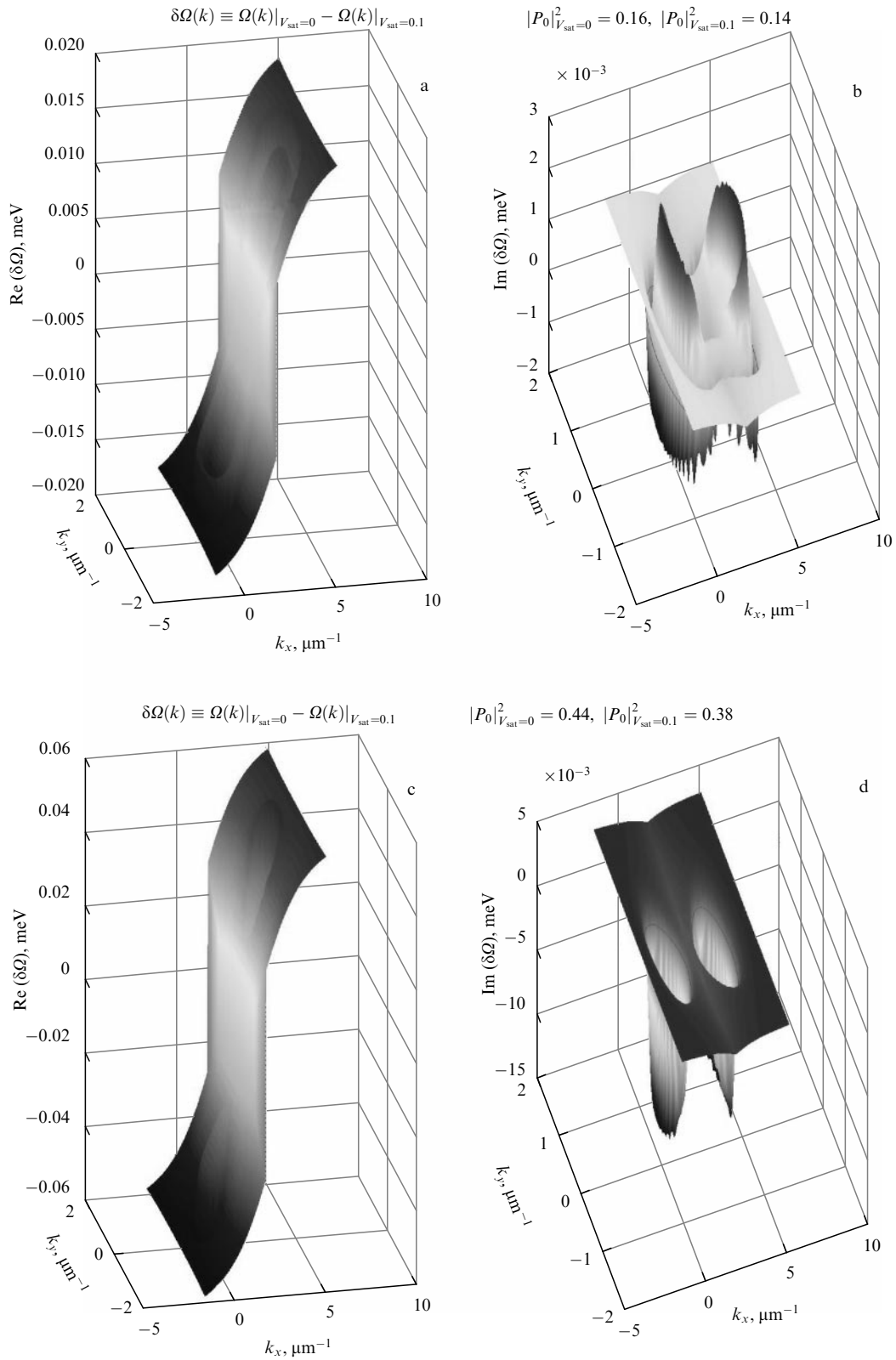

Figure 6. Calculated changes of real (a, b) and imaginary (c, d) parts of the renormalized spectra of the signal and idler modes, taking saturation into account. Figures a, b show spectral changes at the points of the lost stability of the lower branch of the S-curve (shown by the triangles in Fig. 4); Figures c, d correspond to the states with the same external field values but much higher polarization (shown by the star symbol in Fig. 4). The renormalized spectra in Figures a, b are computed for the induced exciton polarization and external field intensity $|\mathcal{P}_0|^2 = 0.16$, $\mathcal{E}^2_{ext} = 0.083$ (for $V_{sat} = 0$) and 0.14, 0.072 (for $V_{sat} = 0.1$); the same parameters in Figures c, d are 0.44, 0.083 (for $V_{sat} = 0$) and 0.38, 0.072 (for $V_{sat} = 0.1$). The scale along the vertical axis on these 'differential' spectra is much smaller than in Fig. 5, showing the spectrum itself, which suggests the weak effect of saturation on the spectral rearrangement at the characteristic points of the S-curve.

trajectory depicting the behavior of the excited mode in Fig. 2). In the case of an empty MC, whose dispersion curve has no inflection point, the upper branch is stable [25, 26]. However, a different situation occurs when the MC contains

polaritons; in this case, the upper branch may be unstable (see the transition at $t \approx 700$ ps in Fig. 2). The cause of this second instability can be understood from Fig. 5c, d, showing the dispersion of eigenfrequencies of the linear problem in (6) and (7) in the absence of saturation calculated for the parameters $|\mathcal{P}_0|^2 = 0.44$ and $|\mathcal{E}_{\rm ext}|^2 = 0.083$, i.e., at the upper branch of the S-contour (see the star symbol on the solid curve in Fig. 4). As follows from Fig. 2, it is approximately this region into which the excited mode falls as a result of the development of the first instability at $t \approx 600$ ps. Then, the regions near $k_{\rm s} \approx 0$, $k_{\rm i} \approx 2k_{\rm p}$ (as shown in Fig. 5d) are characterized by very strong parametric instability with a large incremental growth. Unlike the figure eight during parametric scattering of polaritons on the lower branch of the S-contour [7, 32], the scattered signal on the upper branch of the S-contour reaches its maximum within compact solid angles inside the figure eight, close to $k_{\rm s} \approx 0$, $k_{\rm i} \approx 2k_{\rm p}$. This qualitatively agrees with experimental findings [13, 15]. Owing to the development of the second instability, the solution with a single macro-occupied mode decays: other polariton modes are rapidly populated (see also Fig. 3). As a result, the amplitude of the excited polariton abruptly decreases, and this state turns out to be more or less stable even if fluctuating in time because of rescattering on other polariton modes.

It must be noted in addition that taking the finiteness of saturation $V_{\rm sat} = 0.1$ into account leads to a quantitatively different position of the S-curve (cf the solid and dashed curves in Fig. 4) but does not cause a qualitative change in the scattering scenario. This follows, for example, from the smallness of the difference between the eigenfrequencies of the linear problem (6), (7) for $V_{\rm sat} = 0$ and $V_{\rm sat} = 0.1$ calculated at characteristic jump points on the corresponding S-curve (see Fig. 6).

To summarize, using a simplified quasi-one-dimensional model of polariton – polariton scattering in MCs, we have numerically demonstrated the feasibility of a hard-threshold stimulation of polariton – polariton scattering while smoothly varying the external pump. This is possible due to the mutual influence of bistability of the response of the excited polariton mode and its instability relative to parametric pump. The resultant scattered signal proves to be directed roughly normally to the microcavity, $k_{\rm s} \approx 0$, in qualitative agreement with experiment [13, 15]. The analysis of stability of polariton – polariton scattering indicates that this result must be preserved when taking the quasi-two-dimensionality of the scattering and excitonic saturation into account. In conclusion, we emphasize that an essential condition for the existence of an instability region on the upper branch of the S-shaped curve of a nonlinear oscillator with respect to the scattering into other polariton modes is the presence of an inflection point at the lower polariton dispersion branch. In the case of an empty MC with a quadratic dispersion or pump far away from the inflection region, there is no such instability, and the behavior of the system proves simply bistable.

The authors are grateful to P V Elyutin and N S Maslova for helpful discussions. The work was supported in part by the RFBR and INTAS.

References

1. Savvidis P G et al. *Phys. Rev. Lett.* **84** 1547 (2000)
2. Houdré R et al. *Phys. Rev. Lett.* **85** 2793 (2000)
3. Ciuti C et al. *Phys. Rev. B* **62** R4825 (2000)
4. Tartakovskii A I, Krizhanovskii D N, Kulakovskii V D *Phys. Rev. B* **62** R13298 (2000)
5. Stevenson R M et al. *Phys. Rev. Lett.* **85** 3680 (2000)
6. Baumberg J J et al. *Phys. Rev. B* **62** R16247 (2000)
7. Ciuti C, Schwendimann P, Quattropani A *Phys. Rev. B* **63** 041303 (2001)
8. Whittaker D M *Phys. Rev. B* **63** 193305 (2001)
9. Savvidis P G et al. *Phys. Rev. B* **64** 075311 (2001)
10. Saba M et al. *Nature* **414** 731 (2001)
11. Savasta S, Di Stefano O, Girlanda R *Phys. Rev. Lett.* **90** 096403 (2003)
12. Huynh A et al. *Phys. Rev. Lett.* **90** 106401 (2003)
13. Kulakovskii V D et al. *Nanotechnology* **12** 475 (2001)
14. Kulakovskiĭ V D et al. *Usp. Fiz. Nauk* **175** 334 (2005) [*Phys. Usp.* **48** 312 (2005)]
15. Butté R et al. *Phys. Rev. B* **68** 115325 (2003)
16. Gippius N A et al., in *Proc. of the 26th Intern. Conf. on the Physics of Semiconductors, Edinburgh, UK, 29 July – 2 August 2002* (Institute of Physics Conf. Ser., No. 171, Eds A R Long, J H Davies) (Bristol: IOP Publ., 2003) p. G4-6
17. Kulakovskiĭ V D et al. *Usp. Fiz. Nauk* **173** 995 (2003) [*Phys. Usp* **46** 967 (2003)]
18. Gippius N A et al. *Europhys. Lett.* **67** 997 (2004)
19. Gippius N A, Tikhodeev S G *J. Phys.: Condens. Matter* **16** S3653 (2004)
20. Baas A et al. *Phys. Rev. A* **69** 023809 (2004)
21. Whittaker D M, in *Proc. of PLCMN4, St. Petersburg, June 2004* (2004)
22. Carusotto I, Ciuti C *Phys. Rev. Lett.* **93** 166401 (2004)
23. Tikhodeev S G et al. *Phys. Rev. B* **66** 045102 (2002)
24. Tassone F, Yamamoto Y *Phys. Rev. B* **59** 10830 (1999)
25. Firth W J, Scroggie A J *Phys. Rev. Lett.* **76** 1623 (1996)
26. Kuszelewicz R et al. *Phys. Rev. Lett.* **84** 6006 (2000)
27. Vladimirov A G et al. *Phys. Rev. E* **65** 046606 (2002)
28. Duffing G *Erzwungene Schwingungen bei veränderlicher Eigenfrequenz* (Braunschweig: Vieweg, 1918)
29. Luchinsky D G, McClintock P V E, Dykman M I *Rep. Prog. Phys.* **61** 889 (1998)
30. Gilmore R *Rev. Mod. Phys.* **70** 1455 (1998)
31. Baas A et al. *Phys. Rev. B* **70** 161307(R) (2004)
32. Langbein W *Phys. Rev. B* **70** 205301 (2004)

PACS numbers: **42.65.–k**, **71.36.+c**, **78.65.–n**
DOI: 10.1070/PU2005v048n03ABEH002126

Stimulated polariton – polariton scattering in semiconductor microcavities

V D Kulakovskii, D N Krizhanovskii,
M N Makhonin, A A Demenev,
N A Gippius, S G Tikhodeev

Mixed exciton – photon states in planar semiconductor microcavities (MCs) with quantum wells (QWs) in a $1-3\,\lambda$ thick active layer (where λ is the wavelength of light) represent a new class of quasi-two-dimensional particles having unique properties [1]. Such states, called microcavity polaritons, are realized in MCs if the decay of both the photon and exciton modes does not exceed the exciton – photon interaction energy. Light quantization in a planar MC perpendicular to the plane of the mirrors leads to an almost parabolic dispersion of the photon mode with a very small effective mass near zero lateral quasi-momentum **k**,

$$E_{\rm C} = \left(E_{\rm C}^2(0) + \frac{(\hbar c k)^2}{\varepsilon} \right)^{1/2}, \qquad (1)$$